Progress In Electromagnetics Research M, Vol. 98, 45–54, 2020

Temperature Field Analysis and Optimization of Radial 2-DOF Hybrid Magnetic Bearing

Xun Zhou[1, *], Yangyang Shen[2], and Min Wang[2]

Abstract—The loss of magnetic bearing in the process of operation will lead to the temperature rise of the bearing and affect its performance. A permanent magnet is used to provide bias magnetic flux for hybrid magnetic bearing, which can reduce the loss and temperature rise of the magnetic bearing. In this paper, the loss of radial 2-DOF hybrid magnetic bearing (HMB) is analyzed. On this basis, the 3D thermal analysis model of HMB is constructed by using ANSYS Workbench finite element software. The loss is introduced into the temperature field as a heat source, and the temperature distribution of magnetic bearing is calculated. Combined with the results of loss and temperature analysis, the structural parameters were optimized by using genetic particle swarm optimization algorithm (GAPSO). The results show that the loss and temperature rise of the optimized magnetic bearing are significantly reduced.

1. INTRODUCTION

The magnetic suspension bearing is a new type of support technology that uses non-contact magnetic force to stably suspend the rotor. It has the advantages of no mechanical contact, no friction, no lubrication, long life, etc. [1–3] and is widely used in satellite attitude control, flywheel energy storage [4, 5], aerospace, high-speed machine tools, and vacuum ultra-clean [6]. Compared with traditional bearings, MB has many advantages, but its heating is a problem that cannot be ignored. Especially for a flywheel system supported by MB, the working environment is high vacuum environment, and the heat dissipation condition is poor. The heat generated by loss will affect the normal operation of flywheel, so it is necessary to analyze the loss and temperature field when designing the MB.

Many scholars have conducted research on the loss and temperature field of MBs. In [7], Meeker et al. studied an analytical solution of rotor rotation loss including hysteresis loss and eddy current loss, and compared with the experimental data to verify the accuracy of the analytical solution. Ref. [8] found that the total loss of hybrid radial magnetic bearings was higher than that of radial active magnetic bearings at the same rotational speed. Ref. [9] presented an analysis method for calculating the loss of active magnetic bearings (AMB) based on reluctance network method. This method can estimate the loss of AMB quickly and reduce the development time and workload. In [10], the temperature field of radial magnetic bearings was numerically analyzed by using Ansys thermal analysis module. Based on the conduction and convection heat transfer methods, the thermal analysis model of the radial magnetic bearing is established, and the temperature of the radial magnetic bearing is obtained. The field distribution and temperature field distribution of the radial magnetic bearing were measured by an infrared thermal imager. The experimental values were basically consistent with the temperature values obtained by the analysis. In [11], a loss and temperature field calculation method considering

Received 11 August 2020, Accepted 26 October 2020, Scheduled 30 October 2020
* Corresponding author: Xun Zhou (ZX13000@126.com).
[1] Nanjing Tech University PuJiang Institute, Nanjing 211200, China. [2] Anhui Technical College of Mechanical and Electrical Engineering, Wuhu 241002, China.

electromagnetic coupling and temperature coupling was proposed, and two motors with a power system of 30 kW and a rotational speed of 36000 rpm were developed. The validity and accuracy of the method were verified. However, the above literature has not considered the working environment and operating state of the MB temperature analysis.

In this paper, a radial 2-DOF hybrid magnetic bearing is studied. Firstly, the loss distribution of the magnetic bearing is obtained. Then, the 3D thermal analysis model of HMB is established by using finite element analysis software. The loss of magnetic bearing is introduced into the temperature field as heat source, and the temperature distribution of magnetic bearing is calculated. Finally, based on the analysis of loss and temperature field, the structural parameters of magnetic bearing are optimized. Through optimization, the loss and temperature rise of the magnetic bearing are reduced, so the stability of the magnetic bearing is improved.

2. LOSS ANALYSIS OF HMB

2.1. Loss Calculation of HMB

The HMB uses a permanent magnet (PM) to provide bias flux, which effectively reduces excitation loss. Its losses mainly include iron loss, copper loss, eddy current loss of PM, additional loss, etc. [12–15]. In the stable operation of the magnetic bearing, only the iron loss caused by the change of the magnetic field exists.

2.1.1. Iron Loss

The iron loss is an important part of magnetic bearing, mainly distributed in the rotor and stator. At present, most of the simplified calculation of iron loss is based on Bertotti model, which has been widely used because of its high calculation accuracy and accurate calculation results. According to Bertotti theory, iron loss can be divided into eddy current loss and hysteresis loss. When skin effect and harmonic effect are ignored, the calculation formula of iron loss is as follows

$$P_{Fe} = P_h + P_{et} \tag{1}$$

where P_h is hysteresis loss, and P_{et} is the eddy current loss.

Among them, the iron loss on the rotor is caused by the change of flux density B in the core components. For high-speed applications, eddy current loss is the main part. The iron loss of stator is caused by the change of flux density and control current. When the magnetic bearing is in stable suspension state, the control current is zero, the flux density unchanged, and the iron loss very small. The iron loss of MBs can be divided into eddy current loss and hysteresis loss, and its expression is

$$P_{Fe} = P_{et} + P_h = \frac{1}{6\rho}\pi^2 e^2 f_r^2 B_m^2 V_{Fe}\gamma_{Fe} + k_h f_r B_m^{1.6} V_{Fe}\gamma_{Fe} \tag{2}$$

where P_{Fe} is the core loss of the MB, P_{et} the eddy current loss, P_h the hysteresis loss, ρ the unit resistance of the iron core, e the lamination thickness of the silicon steel sheet, f_r the re-magnetization frequency of the magnetic field in the air gap, B_m the magnitude of the alternating magnetic induction, V_{Fe} the volume of the core, γ_{Fe} the density of the core material, and k_h the hysteresis loss factor. For HMB, the arrangement of magnetic poles is NSNSNSNS. When the rotor is magnetized four times in the process of rotating one cycle, the re-magnetization frequency is 4 times of the rotating frequency [11]. Therefore, the re-magnetization frequency is

$$f_r = 4 \times f_0 \tag{3}$$

where f_0 is the rotation frequency of the rotor.

2.1.2. Copper Loss

The copper loss of HMB is caused by the control current through the winding resistance when the magnetic bearings are disturbed. According to Ohm's law, the formula for calculating the copper loss is as follows

$$P_{cu} = i^2 R = i^2 N \frac{\rho_{cu} l}{A_{cu}} \tag{4}$$

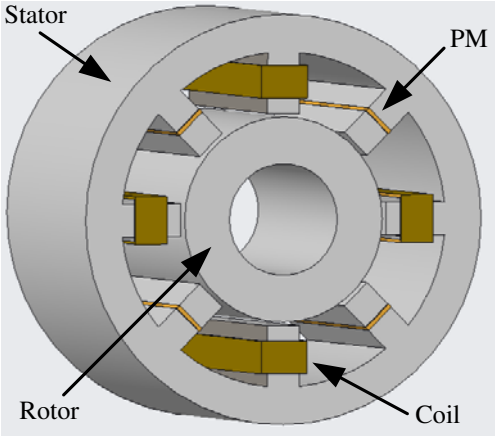

Figure 1. The structure diagram of HMB.

where P_{cu} is the copper loss, i the current flowing through the control coil, R the total resistance of the coil, ρ_{cu} the resistivity of the copper wire, A_{cu} the cross-sectional area of the copper wire, l the average length of the single-turn coil, and N the total number of the coil. For the AMB, the copper current is the sum of the bias current and the control current. For the HMB, the bias magnetic flux is provided by the PM, so the current is only the control current when calculating the copper loss. The structure of HMB is shown in Figure 1.

The structural parameters of HMB are shown in Table 1.

Table 1. Structural parameters of HMB.

Parameter	Value	Parameter	Value
outer diameter of stator/mm	55	coil number	40
inner diameter of stator/mm	46	axial length/mm	40
outer diameter of rotor/mm	28	thickness of PM/mm	2
inner diameter of rotor/mm	10	air/mm	0.5
the pole arc of stator/deg	15		

2.2. Finite Element Analysis of Iron Loss

Assuming that the magnetic bearing rotor is in stable state, the core loss is only caused by the changing magnetic field, and there is no core loss caused by the change of control current frequency. When the speed is 30000 rpm, the iron loss distribution of HMB calculated by finite element analysis software is shown in Figure 2. Figure 2(a) shows the iron loss distribution cloud diagram of the stator, and Figure 2(b) shows the iron loss distribution cloud diagram of the rotor.

It can be seen from Figure 2 that when the HMB is running at high speed, its loss is mainly distributed in the rotor part, and the loss of the stator part is less and mainly distributed in the stator teeth part. When the magnetic bearing operates stably, the overall loss of the magnetic bearing is 21.74 W, of which the hysteresis loss is 2.11 W, accounting for 9.7% of the total loss; the eddy current loss is 19.06 W, accounting for 87.7% of the total loss. When the rotor rotates at a high speed, the polarity of the rotor circumferential bias magnetic field does not change, and only the amplitude changes. Therefore, the eddy current loss of the magnetic bearing is greater than the hysteresis loss.

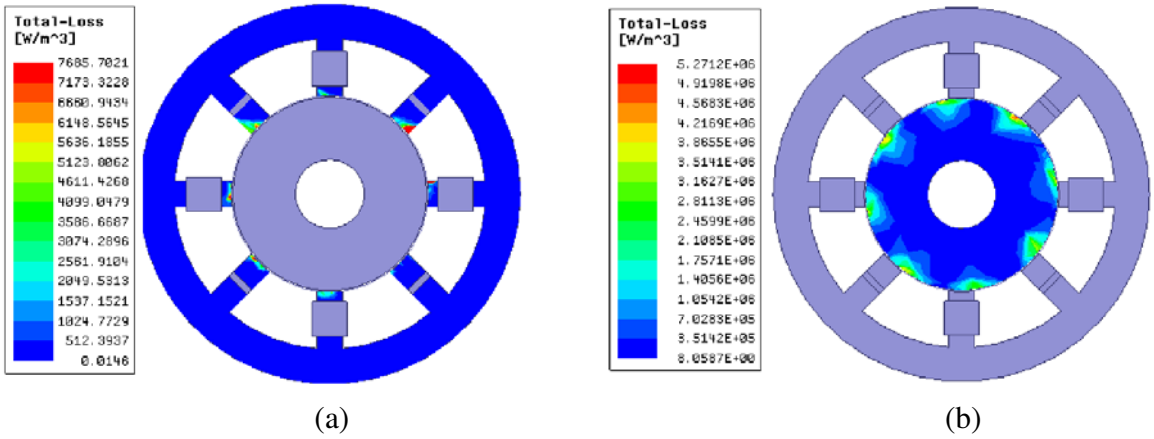

Figure 2. Distribution nephogram of stator and rotor losses. (a) Stator. (b) Rotor.

3. THERMAL ANALYSIS OF HMB

3.1. Thermal Model of HMB

In this paper, the temperature field of magnetic bearing is analyzed by means of Electromagnetic-Thermal unidirectional coupling. Firstly, the thermal model of HMB is established. HMB is composed of a stator, a rotor, a coil, and a PM. In order to simplify the thermal model, several points need to be considered:

(1) The ambient temperature of the magnetic bearing should be kept constant, and the initial temperature of the MB and the temperature of the material should be consistent with the ambient temperature.

(2) Most of the heat generated by the rotor of the magnetic bearing is dissipated through the stator heat conduction and convection heat dissipation. Therefore, the temperature influence of the stator part should be equivalent to a certain ambient temperature consideration when the temperature field simulation is performed.

(3) The winding of magnetic bearing is treated as a heat conducting body. When the winding is equivalent, the volumes of the winding before and after the equivalent are guaranteed to remain unchanged. All the insulation in the stator slot can be equivalent to a thermal conductor.

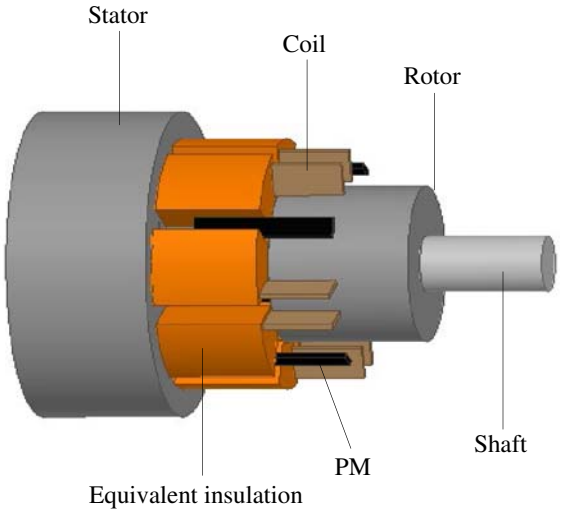

Figure 3. Equivalent thermal model.

(4) The heat dissipation coefficients of the outer surface of the stator and the end faces of the stator are averaged.

Based on the above considerations, the 3D finite element thermal analysis model of the equivalent HMB established in this paper is shown in Figure 3. The winding is equivalent to a thermal conductor, and the winding copper wire paint film, and slot insulation are equivalent to another heat conductor. In order to simplify the calculation, the winding coil is equivalent to a rectangular parallelepiped of the same volume; the insulation between the windings is equivalent to a conductor; and the air gap flowing between the stator and rotor is replaced by a static equivalent air gap.

3.2. Boundary Conditions and Thermal Parameters

Heat transfer is an extremely common process of energy transfer. Due to the temperature difference, heat is transferred from a high temperature object to a low temperature object until temperature equilibrium is reached. According to different heat transfer mechanisms, heat transfer is mainly divided into heat conduction, heat convection, and heat radiation [16].

The heat transfer between objects caused by the change of temperature gradient is heat conduction, which is the main way of heat transfer, and its expression is as follows [17]

$$Q = -\lambda S \frac{dT}{dn} \tag{5}$$

where Q is the heat flux (W), λ the thermal conductivity (W/(m·K)), S the heat transfer area (m^2), and $\frac{dT}{dn}$ the temperature gradient (K/m).

Thermal convection refers to the relative motion between the fluid with a higher temperature and the fluid with a lower temperature, resulting from the heat transfer phenomenon caused by the relative displacement and temperature difference. The process is divided into two categories: natural convection and forced convection. Its expression is

$$Q = hS\left(t_s - t_r\right) \tag{6}$$

where h is the convective heat dissipation coefficient (W/(mm·K)), t_s the material surface temperature (K), and t_r the fluid temperature (K).

Thermal radiation refers to the process in which an object transmits heat by emitting electromagnetic energy. Thermal radiation does not need any medium, and the thermal radiation efficiency in vacuum is the highest. The heat transfer between the two radiation surfaces can be expressed as follows

$$\Phi_{1,2} = \frac{\sigma_b\left(T_1^4 - T_2^4\right)}{\dfrac{1-\varepsilon_1}{\varepsilon_1 A_1} + \dfrac{1}{A_1 X_{1,2}} + \dfrac{1-\varepsilon_2}{\varepsilon_2 A_2}} \tag{7}$$

where $\Phi_{1,2}$ is the heat transfer between the radiation surface 1 and 2; ε_1 and ε_2 are the emissivities of radiation surfaces 1 and 2; A_1 and A_2 are the surface areas of the radiation surfaces 1 and 2; $X_{1,2}$ is the angular coefficients of adiation surfaces 1 and 2 (representing the ratio of the radiation energy absorbed by surface 1 to the total radiation energy emitted by surface 2); σ_b is the blackbody radiation constant; T_1 and T_2 are the temperatures of radiation surfaces 1 and 2.

When determining the thermal parameters of HMB, it is assumed that the thermal conductivity of each component does not change with the temperature. The HMB winding is made of multi-strands of enameled copper wire. In order to simplify the calculation, it is equivalent to a heat conducting body, and its equivalent thermal conductivity is calculated as follows [18]

$$\lambda_{eq} = \lambda_{cu} F_{ew} + \lambda_{imp}(1 - F_{ew}) \tag{8}$$

where λ_{cu} is the thermal conductivity of copper, λ_{imp} the thermal conductivity of the insulating material, and F_{ew} the tank full rate. The thermal conductivity of each part of the material is calculated as shown in Table 2.

Table 2. Thermal parameters of materials.

Assembly of bearing	Density (kg/m^3)	Specific heat capacity (J/kg·K)	Thermal conductivity (W/(m·K))
Stator and rotor	7800	465	52
Insulating materials	1700	1340	0.326
copper	8900	390	380
Shaft	7700	480	50.2
PM	8300	540	10

3.3. Analysis of Simulation Results

In this paper, the magnetic thermal coupling transient analysis of magnetic bearing is carried out by using ANSYS Workbench. The loss of magnetic bearing is calculated by electromagnetic analysis, and then the loss is loaded into the transient temperature field as a heat source to obtain the temperature distribution of each component of magnetic bearing. Figure 3 shows the temperature distribution

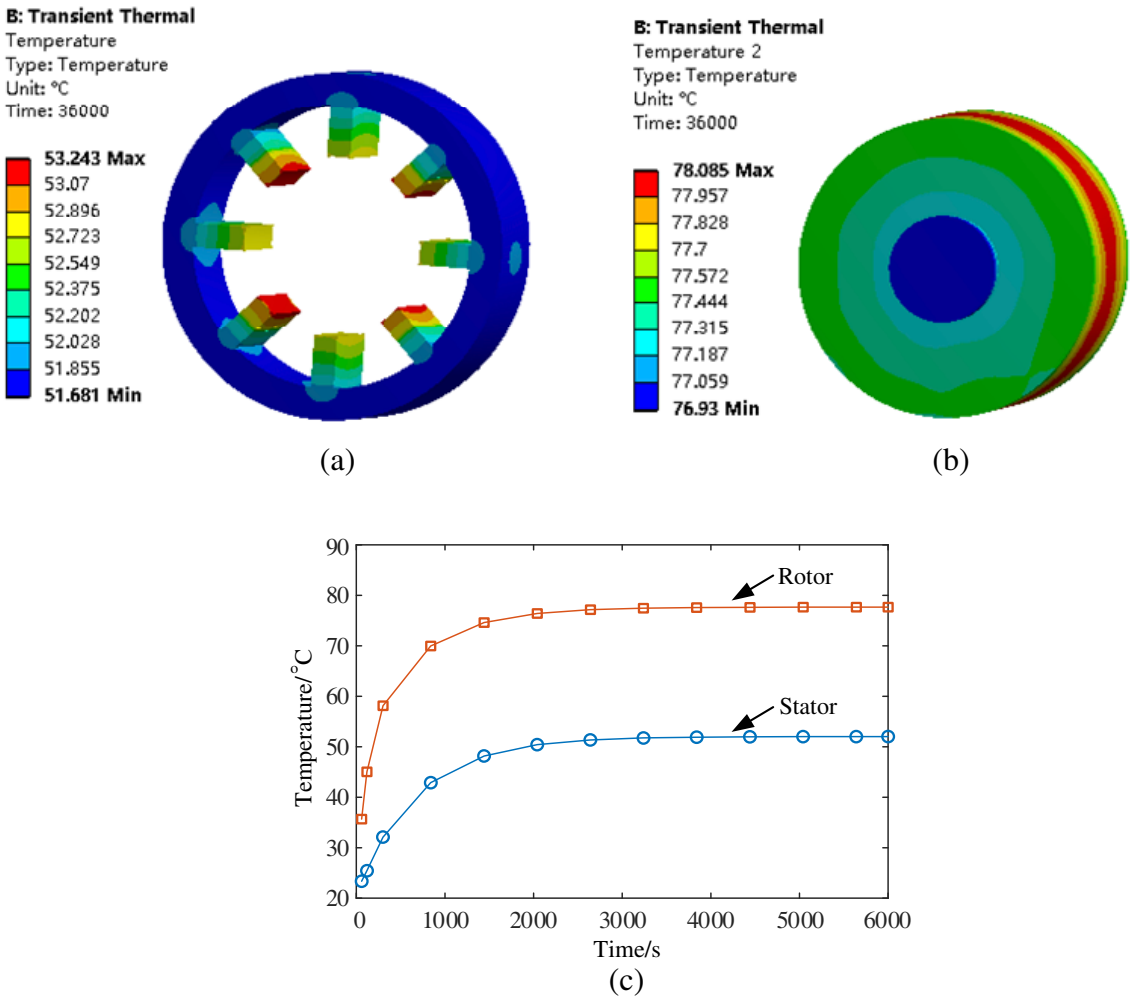

Figure 4. Temperature variation curve of each component. (a) Stator. (b) Rotor. (c) Temperature rise curve.

nephogram and curve of magnetic bearing under stable operation condition. It can be seen from the figure that the temperature of the rotor is significantly higher than the stator. And the temperature of the stator tooth is higher than that of the stator yoke, which is consistent with the loss distribution.

It can be seen from Figure 4 that the temperature of HMB rises rapidly at the beginning of operation, because the temperature of magnetic bearings is not different from that of external environment. The heat generated by the loss of HMB is used to heat itself, and the heat dissipation to external environment is small. After a period of operation, the temperature of HMB is quite different from that of external environment. The stator begins to dissipate heat through heat conduction and heat radiation; the rotor radiates heat through heat radiation; the temperature of HMB rises slowly.

4. OPTIMIZATION DESIGN OF HMB

4.1. Optimal Design

Through the analysis in the previous section, the loss and temperature rise distribution of HMB are obtained. The rise of the magnetic bearing temperature will inevitably lead to the decline of its performance, so it is necessary to optimize the structural parameters. The main function of HMB is to provide enough controllable suspension force so that the rotor can be stably suspended in the balance position. The suspension force provided by magnetic bearing should be as large as possible. The increase of suspension force will inevitably lead to the increase of the volume and axial length. The increase of axial length and volume will increase the loss and temperature of magnetic bearing. Therefore, there are contradictions between the performance of magnetic bearings. In order to optimize the comprehensive performance of magnetic bearings, this paper takes the minimum loss and volume as the optimization objectives and uses the optimization algorithm to optimize the HMB.

Optimization objective: V and iron loss P_{Fe} of magnetic bearing, the volume calculation formula is

$$V = V_r + V_s + V_{pm} \tag{9}$$

where V_r is the volume of the rotor, V_s the volume of the stator, and V_{pm} the volume of the permanent magnet.

The design variables of magnetic bearing are shown in Figure 5. According to the core loss calculation model, the core loss of HMB is closely related to iron core volume, magnetic density amplitude, and magnetization frequency. The larger the core volume is, the greater the amplitude of magnetic flux density, the faster the magnetization frequency, and the greater the iron loss is. The change of air gap length and stator pole width will affect the magnetic flux density amplitude B and magnetization frequency, which will lead to the change of magnetic bearing core loss. Therefore, the air gap length and magnetic pole width are closely related to the loss, so they are taken as optimization variables.

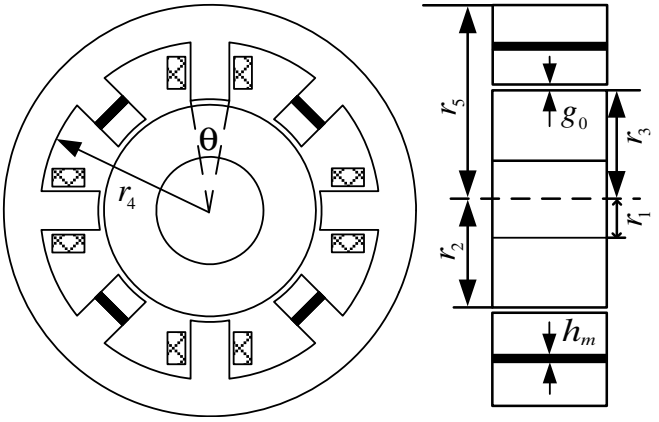

Figure 5. Design variables of HMB.

Constraints: according to the design experience, geometric rules, and considering the practical application environment, the design variables of HMB should meet the following constraints

$$\begin{cases} r_5 - r_4 > 0 & r_2 - r_1 > 0 \\ r_4 - r_3 > 0 & r_4 - r_2 - g_0 > 0 \\ r_3 - r_2 > 0 & g_0 \geq 0.3 \\ B_c \leq 0.6 & B_0 \leq 0.6 \\ B_{\max} \leq 1.2 & \end{cases} \tag{10}$$

4.2. Analysis of Optimization Results

After determining the optimization objective function, design variables, and constraints, the GAPSO is used to optimize the main parameters of the HMB. The results of the design variables and optimization objectives of the HMB before and after optimization are shown in Table 3.

Table 3. Results before and after optimization.

Parameters	Initial value	Optimization value
r_5/mm	55	50
r_4/mm	46	41.3
r_2/mm	28	26.7
g_0/mm	0.5	0.5
h_m/mm	2	2.2
l/mm	40	36
θ	15	19.5
F/N	105	128.8
V/m^3	2.534E-4	1.976E-4
P/W	21.74	18.7

By analyzing the data in the table, the suspension force of the optimized magnetic bearing increases by 18.5% from 105N to 128.8N; the volume decreases from 2.534E-4m^3 to 1.976E-4m^3, decreasing by 22%; and the loss decreases from 21.74 W to 18.7 W, decreasing by 14%. In order to verify the rationality and effectiveness of the optimization, the 3D temperature field analysis model is established by using the optimized structural parameters, and the temperature field of the optimized magnetic bearing is analyzed. Figure 6 shows the optimized temperature distribution cloud of HMB.

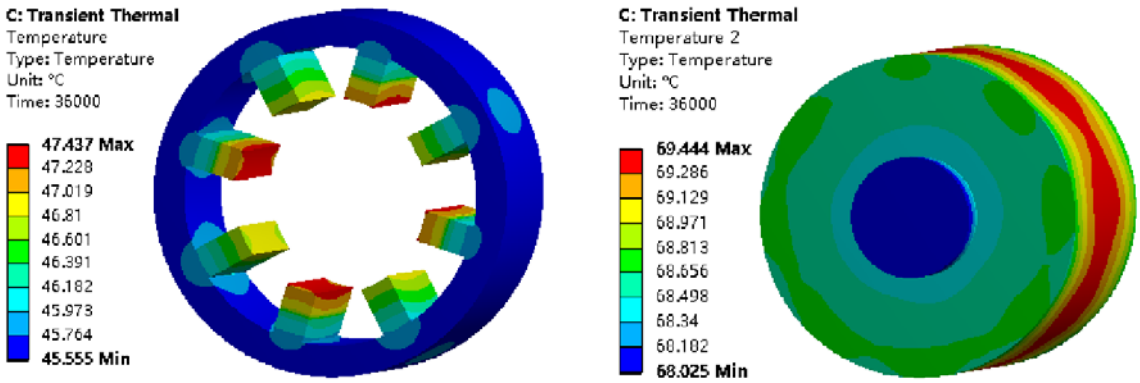

(a) (b)

Figure 6. Temperature distribution cloud diagram of HMB after optimization. (a) Stator. (b) Rotor.

Figure 7 shows the temperature change curve of the stator and rotor of the HMB after optimization. It can be seen from Figure 6 and Figure 7 that the temperature of the stator and rotor of the hybrid magnetic bearing after optimization is significantly reduced. The temperature of the stator is reduced by about 6°C, and the temperature of the rotor is reduced by about 10°C. The temperature reduction of the HMB can effectively improve the stability of the magnetic bearing operation.

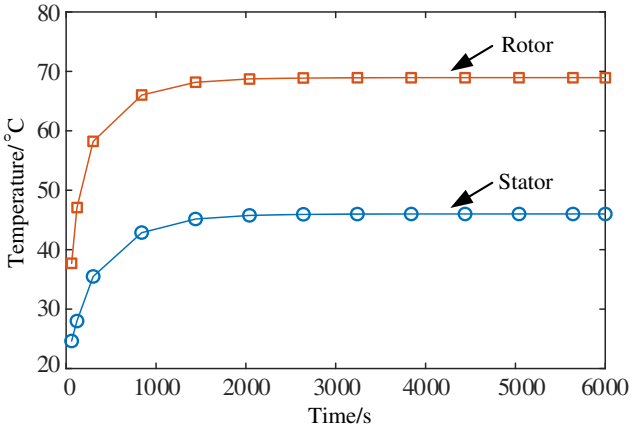

Figure 7. Temperature rise curve of HMB.

5. CONCLUSION

In this paper, the loss calculation of radial 2-DOF hybrid magnetic bearing is analyzed. On this basis, the finite element analysis software is used to verify the loss. By introducing the loss into the temperature field as a heat source, the temperature is simulated and analyzed. The simulation results show that the loss of HMB is mainly distributed in the rotor, and the rotor temperature is significantly higher than the stator temperature. In order to reduce the loss and temperature rise of magnetic bearing, the structural parameters of HMB are optimized by GAPSO on the basis of the above analysis. After optimization, the loss and temperature of the magnetic bearing are significantly reduced.

REFERENCES

1. Santra, T., D. Roy, A. B. Choudhury, and S. Yamada, "Vibration control of a hybrid magnetic bearing using an adaptive sliding mode technique," *Journal of Vibration and Control*, Vol. 24, No. 10, 1848–1860, 2018.
2. Huang, Z., J. Fang, X. Liu, et al., "Loss calculation and thermal analysis of rotors supported by active magnetic bearings for high-speed permanent-magnet electrical machines," *IEEE Transactions on Industrial Electronics*, Vol. 63, No. 4, 2027–2035, 2016.
3. Santra, T., D. Roy, and A. B. Choudhury, "Calculation of passive magnetic force in a radial magnetic bearing using general division approach," *Progress In Electromagnetics Research M*, Vol. 54, 91–102, 2017.
4. Wang, Z., T. Zhang, and S. Wu, "Suspension force analysis of four-pole hybrid magnetic bearing with large radial bearing capacity," *IEEE Transactions on Magnetics*, Vol. 56, No. 8, 2020.
5. Le, Y., J. Sun, and B. Han, "Modeling and design of 3-DOF magnetic bearing for high-speed motor including eddy-current effects and leakage effects," *IEEE Transactions on Industrial Electronics*, Vol. 63, No. 6, 3656–3665, 2016.
6. Han, B., S. Zheng, Y. Le, et al., "Modeling and analysis of coupling performance between passive magnetic bearing and hybrid magnetic radial bearing for magnetically suspended flywheel," *IEEE Transactions on Magnetics*, Vol. 49, No. 10, 5356–5370, 2013.

7. Meeker, D. C., A. V. Filatov, and E. H. Maslen, "Effect of magnetic hysteresis on rotational losses in heteropolar magnetic bearings," *IEEE Transactions on Magnetics*, Vol. 40, No. 5, 3302–3307, 2004.
8. Bakay, L., M. Dubois, P. Viarouge, et al., "Losses in hybrid and active magnetic bearings applied to long term flywheel energy storage," *International Conference on Power Electronics*, IET, 2010.
9. Romanenko, A., A. Smirnov, R. P. Jastrzebski, et al., "Losses estimation and modelling in active magnetic bearings," *European Conference on Power Electronics & Applications*, 2014.
10. Zeisberger, M., T. Habisreuther, D. Litzkendorf, et al., "Optimization of levitation forces in superconducting magnetic bearings," *IEEE Transactions on Applied Superconductivity*, Vol. 11, No. 1, 1741–1744, 2001.
11. Xin, L. and C. Wu, "Temperature field analysis and calculation of radial magnetic bearings," *Machinery*, Vol. 49, No. 6, 18–21, 2011.
12. Ren, X., Y. Le, B. Han, and K. Wang, "Loss and thermal estimation method of a magnetic bearing system considering electromagnetic and temperature coupling," *International Conference on Electrical Machines & Systems*, IEEE, 2017.
13. Shelke, S. and R. V. Chalam, "Optimum energy loss in electromagnetic bearing," *Proceedings of the IEEE*, 374–379, 2011.
14. Han, B. C., Z. He, X. Zhang, et al., "Loss estimation, thermal analysis and measurement of a large-scale turbomolecular pump with active magnetic bearings," *IET Electric Power Applications*, Vol. 14, No. 7, 1283–1290, 2020.
15. Zhai, L., B. Han, X. Liu, et al., "Losses estimation, thermal-structure coupled simulation analysis of a magnetic-bearing reaction wheel," *International Journal of Applied Electromagnetics and Mechanics*, 1–20, 2018.
16. Romanenko, A., A. Smirnov, R. P. Jastrzebski, and O. Pyrhonen, "Losses estimation and modelling in active magnetic bearings," *European Conference on Power Electronics & Applications*, IEEE, 2014.
17. Sun, Y., B. Zhang, Y. Yuan, and F. Yang, "Thermal characteristics of switched reluctance motor under different working conditions," *Progress In Electromagnetics Research M*, Vol. 74, 11–23, 2018.
18. Liu, C., X. Zhu, Y. Du, et al., "Design and performance analysis of magnetic field modulated flux-switching permanent magnet machine based on electrical-thermal bi-directional coupling design method," *Proceedings of the CSEE*, Vol. 37, No. 21, 6237–6245, 2017.